Hurdiid radiodontans from the middle Cambrian (Series 3) of Utah

Stephen Pates[1], Allison C. Daley[1,2,3], and Bruce Lieberman[4,5]

[1]Department of Zoology, University of Oxford, Oxford, OX1 3PS, UK
<stephen.pates@zoo.ox.ac.uk>
[2]Oxford University Museum of Natural History, Oxford, OX1 3PW, UK
[3]Faculty of Geosciences and Environment, University of Lausanne, Sorge Géopolis, CH1015, Lausanne, Switzerland <allison.daley@unil.ch>
[4]Division of Invertebrate Paleontology, Biodiversity Institute, University of Kansas, Lawrence, KS 66045, USA <blieber@ku.edu>
[5]Department of Ecology and Evolutionary Biology, University of Kansas, Lawrence, KS 66045, USA

Running Header: Hurdiids from the middle Cambrian of Utah

Abstract.—Radiodontan body elements, some belonging to *Peytoia* and *Hurdia* and some unassigned, have been reported from the Langston Formation (Spence Shale Member), Wheeler Formation, and Marjum Formation of the middle Cambrian (Series 3) of Utah. These identifications are reassessed in light of recent work on the morphology of the radiodontan *Hurdia*. New specimens of *Hurdia* are identified from the Spence Shale, representing mouthparts (oral cones), cephalic carapace H-elements, frontal appendages and a single isolated swimming flap. The shape of the H-elements allows *H. victoria* to be identified from the Spence Shale for

the first time. The flap is larger and more complete than any reported from the Burgess Shale, and allows for a better understanding of the morphology of *Hurdia* swimming flaps. A 3D model of a *Hurdia* frontal appendage indicates that there is only one morph of *Hurdia* frontal appendage found in both species, and apparent morphological differences between disarticulated appendages reflect a preservational continuum caused by varying oblique angles relative to the seafloor. *Peytoia* should no longer be reported from the Spence Shale, but its presence is confirmed in the Wheeler and Marjum formations. New mouthparts (oral cones) of *Hurdia* from the Spence Shale and *Peytoia* from the Marjum Formation with surface textures of sub-millimeter diameter raised nodes are described. These new features have not been observed in material from the Burgess Shale, and suggest slight differences in preservation.

Introduction

Our understanding of the morphology and systematics of *Hurdia* Walcott, 1912 has greatly expanded in recent years, and it is now recognized as a significant taxon within Radiodonta present in several of the well-known Cambrian soft-bodied biotas including: the Burgess Shale in Canada and the nearby Stanley Glacier, Marble Canyon, Tulip Beds and Mount Stephen sites (Daley et al., 2009; 2013a); the Jince Formation in the Czech Republic (Chlupáč and Kordule, 2002, fig. 7); Wheeler Formation (Robison and Richards, 1981, pl. 4, fig. 1a,b) and the Spence Shale (Daley et al., 2013a) in Utah, USA; the Shuinjingtuo Formation in China (Cui and Hou, 1990); and the Fezouata Biota in Morocco (Van Roy and Briggs, 2011, figs. 1d–i, S4a–c; 1l, S3c,d, S4f). Notably, the soft-bodied biotas from the middle Cambrian (Series 3) of Utah have yielded a large number of specimens previously identified as radiodontans in general, and

usually *Anomalocaris* Whiteaves, 1892 or *Peytoia* Walcott, 1911 (Daley and Bergström, 2012) (e.g., Conway Morris and Robison, 1982; Briggs and Robison, 1984; Conway Morris and Robison, 1988; Robison, 1991; Briggs et al., 2008), but the systematic position of most of this material has not yet been re-evaluated in light of the new discoveries on *Hurdia*. By analysis of appendages and mouthparts originally described in Conway Morris and Robison (1988) Daley et al. (2013a) were able to conclude that *Hurdia* was in fact present in the middle Cambrian (Series 3) of Utah alongside *Peytoia*, and described four new specimens from the Spence Shale. Herein, we reconsider the identifications of radiodontan specimens from Utah in detail and confirm that *Hurdia* is well represented there. Further, we identify *H. victoria* in the Spence Shale for the first time. A 3D model of an idealized *Hurdia* appendage potentially allows characters used in previous phylogenetic analyses (e.g., Vinther et al., 2014; Cong et al., 2014; Van Roy et al., 2015) to be visualized and evaluated in the hopes of possibly inferring which characters might be influenced by taphonomic factors.

The middle Cambrian (Series 3) of Utah is well known for its soft-bodied deposits that preserve a diverse array of taxa in several different depositional settings (Robison, 1991; Briggs et al., 2008; Gaines et al., 2008, 2012; Brett et al., 2009; Halgedahl et al., 2009). The Gunther family of Utah, along with Richard Robison (Robison, 1965; Gunther and Gunther, 1981), played a pivotal role in helping this treasure trove of fossils come to light. Many significant finds have been made from these deposits over the years (Resser, 1939; Brooks and Caster, 1956; Briggs and Robison, 1984; Babcock and Robison, 1988; Conway Morris and Robison, 1986, 1988; Robison and Wiley, 1995; Briggs et al., 2005), and new discoveries continue to be made (Robison and Babcock, 2011; Stein et al., 2011; Conway Morris et al., 2015; LoDuca et al., 2015; Robison et al., 2015). Taxa from these deposits have also provided insights into higher-

level arthropod relationships (Hendricks and Lieberman, 2008) while forming a core source of data used to study paleobiogeographic and macroevolutionary patterns during the Cambrian radiation interval (Hendricks et al., 2008).

Non-hurdiid radiodontans reported from the Langston Formation (Spence Shale Member), Wheeler Formation and Marjum Formation are limited to two body fossils of *Anomalocaris*: one from the Spence Shale and one from the Wheeler Formation, both described by Briggs et al. (2008, figs. 1, 3). Neither specimen has well preserved large frontal appendages, and the two specimens seem to represent two different and new species. Isolated appendages of *Anomalocaris* aff. *canadensis* Whiteaves, 1892, and *Anomalocaris*? sp. from the younger (Guzhangian) Weeks Formation in Utah have been described by Lerosey-Aubril et al. (2014). No new *Anomalocaris* appendages or bodies were identified during the course of this study. We emphasize new findings relating to *Hurdia* and *Peytoia*.

As is the case for other radiodontans, *Hurdia* and *Peytoia* are found mostly as isolated elements (carapace elements, mouthparts, appendages, and body flaps) and rarely as whole bodies, which can at times make taxonomic identification challenging. In general, the morphology of *Hurdia* can be divided into a head region with a pair of frontal appendages either side of a circular oral cone. The oral cone made up of four large plates, equally spaced, with seven small plates between each pair of large plates; these surround an opening with multiple inner rows of teeth. A large frontal carapace of three sclerotized elements (two lateral P-elements and one dorsal H-element) and stalked eyes complete the head region. The body is made up of seven to nine segments, with reduced swimming flaps and prominent setal structures (Daley et al., 2009; 2013a). A morphometric analysis showed that there are two species of *Hurdia*, *H. victoria* and *H. triangulata*, which are differentiated by comparing the length and width of the

carapace H-element (Daley et al., 2013a). *Hurdia* and *Peytoia* have recently been recovered within Hurdiidae (e.g. Van Roy et al. 2015), but these genera differ in a number of ways. *Peytoia* and *Hurdia* have a similar overall frontal appendage morphology in that both have elongated ventral spines, but these differ in numerous details including the number and length-width ratio of the podomeres, and the shape, arrangement and number of ventral spines (Daley et al., 2013a). *Hurdia* has a complex frontal carapace composed of three sclerite elements, whereas *Peytoia* has no evidence for such a large frontal carapace, with only traces of possible carapace material immediately surrounding the head in ventrally preserved specimens (Daley et al. 2009). The oral cone has the same arrangement of outer plates in *Hurdia* and *Peytoia*, but the multiple inner rows of teeth present in *Hurdia* are absent in *Peytoia*. The body trunk in *Hurdia* consists of seven to nine segments that are more cylindrical than the dorsaventrally flattened body of *Peytoia*, which has 13 body segments. The swimming flaps of *Hurdia* are much smaller than the wide flaps of *Peytoia*, but setal blades are more prominent in *Hurdia* as compared to *Peytoia* (Whittington and Briggs, 1985, fig. 101).

Materials and methods

One body specimen (USNM 374593) is held at the Smithsonian Museum of Natural History, Washington, D.C., USA. The remainder of the material studied is held at the Division of Invertebrate Paleontology, Biodiversity Institute, University of Kansas, Lawrence, USA (KUMIP). Detailed information for the fossil localities are available in Table 3 of Hendricks et al. (2008). All specimen numbers, previous publications and new identifications are provided in Table 1.

Photographs were taken with a Canon EOS 500D DSLR Camera with Canon EF-S 60 mm Macro Lens, controlled for remote shooting using the EOS Utility 2 program. Photographs were taken under cross polarized light, non-polarized light, wet and dry, and under high and low angle lighting. Measurements for calculating RI values, and length:width ratios were taken from digital photographs using ImageJ 2.The 3D model was made using Blender 2.76b. A box model was created from a sketch of *Hurdia* adapted from Daley and Budd (2010). This was modified with a subdivision surface, and rendered to a video. A phylogenetic analysis in TNT v. 1.5 (Goloboff & Catalano, 2016) was run using implicit enumeration under equal weighting on a data matrix modified from Van Roy et al. (2015) consisting of 33 taxa and 61 characters. Modifications to the phylogenetic analysis data matrix were made in Mesquite v. 3.2 (Maddison and Maddison, 2017).

Geologic setting

The Spence Shale Member of the Langston Formation, middle Cambrian Series 3, Stage 5, is a diverse soft-bodied biota (Gunther and Gunther, 1981; Robison, 1991; Liddell et al., 1997), and knowledge of the paleontology, sedimentology, geochemistry, and taphonomy of this deposit has increased substantially over the past few years (Briggs et al., 2008; Garson et al., 2012; Gaines et al., 2012; Olcott Marshall et al., 2012; Gaines, 2014; Kloss et al., 2015). The Spence Shale is primarily made up of shale, with some limestone, and it is developed in a series of parasequences (Liddell et al., 1997; Garson et al., 2012). Detailed discussions of the sedimentology, taphonomy, and geochemistry of the Spence Shale are provided by Liddell et al. (1997), Garson et al. (2012), and Kloss et al. (2015), respectively. All of the specimens from the Spence Shale

discussed herein come from the Wellsville Mountains of northern Utah (Hendricks et al., 2008; Hendricks, 2013).

The Wheeler Formation, Drumian, Cambrian Series 3, from the House Range of Utah is slightly younger than the Spence from the Wellsvile Mountains, and it too contains a diverse soft-bodied biota (Robison, 1964; Gunther and Gunther, 1981; Briggs and Robison, 1984; Rogers, 1984; Rees, 1986; Robison, 1991; Robison et al., 2015). There have been a substantial number of relatively recent sedimentological, taphonomic, and geochemical studies of the soft-bodied biota from this formation and region (e.g., Gaines and Droser, 2003, 2005; Briggs et al., 2008; Brett et al., 2009; Halgedahl et al., 2009; Gaines, 2014). The unit consists of homogeneous mudstones and interbedded mudstones with thin-grained, fine-bedded limestones. The soft-bodied material occurs primarily within carbonaceous shales (Gaines and Droser, 2003, 2005).

The still slightly younger soft-bodied deposits from the Marjum Formation, Drumian, Cambrian Series 3, generally resemble lithologically, stratigraphically and taphonomically those deposits from the Wheeler Formation where it is exposed in the House Range (Elrick and Snider, 2002; Brett et al., 2009; and Gaines and Droser, 2010), although they represent a shallower facies (Briggs and Robison, 1984; Brett et al., 2009).

The relative global chronostratigraphic ages and polymerid trilobite biostratigraphy of Radiodonta-preserving units in Utah and British Columbia can be seen in Figure 1.

Results

Taxonomic identifications of new and previously described material are summarized in Table 1. *Hurdia victoria* Walcott, 1912 is described for the first time from the Spence Shale. *Hurdia* also occurs in the Wheeler Formation. *Peytoia* occurs in the Wheeler and Marjum formations, but should no longer be reported as present in the Spence Shale.

Hurdia from the Spence Shale Member.—Some of the material interpreted as *Hurdia* from the Spence Shale comprise appendages and mouthparts (Figs. 2, 3); these include both previously described specimens (Briggs et al., 2008; Daley et al., 2013a, fig. 24) as well as new material. New carapace material (Fig. 4.1–4.5), which allows identification to the species level, and a large, isolated flap (Fig. 4.6, 4.7) are also discussed here for the first time. In addition, appendages previously interpreted as *Peytoia nathorsti* (Conway Morris and Robison, 1988), are here reinterpreted as belonging to a *Sidneyia*-like taxon.

KUMIP 314145a/b (Fig. 2.1) is a small, single incomplete *Hurdia* appendage with 7 visible podomeres with well-defined boundaries of around 1 mm in thickness. Podomeres at the proximal end of the appendage where the ventral spines attach are not preserved. KUMIP 314178 (Fig. 2.2) is a mostly complete small, single *Hurdia* appendage with ten podomeres separated by clear podomere boundaries of around 1 mm thickness. KUMIP 314040a/b (Fig. 2.3, 2.4) is a small *Hurdia* appendage with nine podomeres. Five large ventral spines, attached to podomeres 2–6, are tightly packed and appear curved forwards, beyond the distal end of the appendage. Auxiliary spines are only visible on the distalmost ventral spine. KUMIP 314042 (Fig. 2.5) is a larger *Hurdia* appendage with ten podomeres with clear podomere boundaries of around 1 mm thickness. The five large, straight ventral spines have slightly curved distal ends.

Briggs et al. (2008) identified KUMIP 312405a/b (Fig. 3 herein) as a pair of radiodontan appendages with mouthparts. The two appendages are preserved with one ('app. 1' in Fig. 3.3) on a higher level of rock than the other ('app. 2' in Fig. 3.3). App. 1 is well preserved and made up of ten podomeres. Large ventral spines are present on podomeres 2–6 and a small ventral spine is visible on podomere 9 ('vs' in Fig. 3.3). A terminal spine is visible on podomere 10 ('ts' in Fig. 3.3). App. 2 is not as clearly visible. The distalmost podomeres are visible. Three large ventral spines are preserved together, with the distal one angled forwards, similar to the overlying appendage. The mouthparts are made up of four large plates ('lp' in Fig. 3.3) arranged at 90° to each other around a rectangular opening. The total number of smaller plates is not clear, as the outer edge of the oral cone is not well preserved, but where it can be counted there are seven smaller plates between the large plates, which extrapolates to a total of 32 plates, four large and 28 small, characteristic of *Hurdia* and *Peytoia*. By contrast, *Anomalocaris* mouthparts have three large plates at 120° (Daley and Bergström, 2012). *Peytoia* mouthparts can be differentiated from *Hurdia* as *Hurdia* has numerous tooth rows in the central opening, whereas in *Peytoia* the central opening lacks tooth rows (Daley and Bergström, 2012). In the central opening of this specimen, additional tooth rows are visible ('tr' in Fig. 3.3), indicating this specimen is a *Hurdia*. The appendages associated with the mouthparts are both consistent with this interpretation, and are likely from the same animal. KUMIP 314175a/b (Fig. 2.6) is a small, oval oral cone of *Hurdia*. It is unusual in that it has small raised nodes (radius 1 mm) visible on one of the large plates and several small plates. KUMIP 314265a/b (Fig. 2.7) is another small *Hurdia* oral cone. The outer margins of the plates are not preserved, but multiple inner rows of teeth in an approximately rectangular central opening are clearly visible. Again, there are some possible small round nodes (radius 1 mm) visible on some plates.

The length:width ratio of H-elements from the carapace of *Hurdia* can be used to distinguish *H. victoria* from *H. triangulata*: *H. victoria* has H-elements with lengths greater than 1.5 times the width (but less than 2.0 times) and *H. triangulata* has H-elements with lengths less than 1.5 the width (Daley et al., 2013a). KUMIP 314039 (Fig. 4.2), KUMIP 314050 (Fig. 4.1, 4.4), and KUMIP 314056 (Fig. 4.3, 4.5), identified by height:width ratios, are the first *H. victoria* specimens identified from the Spence Shale; *H. triangulata* has not yet been identified. Reticulation polygons were observed on parts of the surface of some elements (Fig. 4.4). The specimen illustrated in (Fig. 4.3, 4.5) has ten small brown patches (1–5 mm in radius) and a trilobite with inferred manganese dendrites radiating from it, obscuring parts of the fossil. Similar dendrites with elevated manganese content have been reported from the Pioche Shale (Moore and Lieberman, 2009). Evidence for the two-layered H-element can be seen towards the strengthened tip (Fig. 4.5).

KUMIP 314057a/b (Fig. 4.6, 4.7) is a part and counterpart of an isolated radiodontan swim flap covered with regularly spaced, prominent transverse lines, also referred to as "strengthening rays" (Whittington and Briggs, 1985) or "veins" (Chen et al., 1994; Hou et al., 1995), about 1 mm wide and 2 mm apart. The flap is relatively large compared to Hurdia flaps reported from the Burgess Shale (Daley et al., 2013a), measuring approximately 65 mm in width and 45 mm in height. This specimen is tentatively identified as *Hurdia* because of the presence of transverse lines across the entire surface of the flap, which is not seen in *Peytoia* (where the transverse lines are confined to the anterior half of the flap) or *Anomalocaris* (which lacks transverse lines entirely).

229 *Sidneyia? from the Spence Shale Member*.—Conway Morris and Robison (1988, fig. 26.1a,
230 26.1b, 26.2) identified four specimens (KUMIP 204777–204780) as broken spines of *Peytoia*
231 *nathorsti* appendages. These are reinterpreted as distal podomeres of endopods (walking
232 appendages) of a *Sidneyia*-like taxon, based on the rounded curvature of the overall structure, the
233 oblique angle of the spines, the characteristic arrangement of repetitive bundles of decreasing
234 spine size, and the presence of podomere boundaries faintly visible on some specimens (compare
235 KUMIP 204777–204780: Conway Morris and Robison, 1988, fig. 26.1a, 26.1b, 26.2 to Bruton,
236 1981, figs. 48, 53, 55, 58, 60, 88, 92 and Stein, 2013, fig. 7B–D). This therefore indicates
237 *Peytoia* should no longer be reported as present in the Spence Shale. *Sidneyia* was previously
238 reported from the Spence Shale (Briggs et al., 2008).
239
240 *Hurdiids from the Wheeler Formation*.—*Hurdia* is known from the Wheeler Formation by a
241 single P-element. *Peytoia* is known from one appendage and several mouthparts. KUMIP
242 153901a/b (Fig. 5.6, 5.7) was first described by Robison and Richards (1981, pl., 4, fig. 1a, b) as
243 *Proboscicaris agnosta*, which at the time was thought to be a phyllocarid. *Proboscicaris* is now
244 identified as the P-element of the *Hurdia* carapace (Daley et al., 2009). KUMIP 314086a/b (Fig.
245 5.1, 5.2) was first described by Briggs et al. (2008, fig. 2.2) as a radiodontan appendage. Owing
246 to the relatively limited preservation, they did not classify it to genus. It is an appendage with 10
247 podomeres, with elongated ventral spines on podomeres 2–6. Six auxiliary spines are present
248 perpendicular to the ventral spine of podomere 5. There are three small triangular terminal spines
249 on podomere 10. The presence of three terminal spines, the orientation of ventral spines, and the
250 curved distal end indicate it is a *Peytoia* appendage. Conway Morris and Robison (1982, text-
251 fig. 1, pl. 1 figs. 1–5) described two specimens, KUMIP 153093a/b (Fig. 5.10, 5.11) and KUMIP

252 153094 (Fig. 5.5), of radiodontan oral cones as *Peytoia* cf. *P. nathorsti*, and we support this
253 interpretation based on the overall arrangements of plates, and the lack of tooth rows inside the
254 main opening. The genuine absence of additional rows of teeth can be confirmed by examining
255 the central opening, which well preserved. KUMIP 314078 (Fig. 5.8, 5.9), first described by
256 Briggs et al. (2008, fig. 2.2), is an oral cone with four large plates, and seven smaller plates
257 between each larger plate. Part of the mouth apparatus is not preserved, but it can be inferred that
258 it had 32 plates (four large, 28 small) radially arranged. The central opening of the incomplete
259 mouth apparatus does not have additional tooth rows, so it can be identified as *Peytoia*.
260 Conway Morris and Robison (1988, fig. 26.3) identified KUMIP 204781a/b (Fig. 5.3,
261 5.4) from the Wheeler Formation as a *P. nathorsti* appendage. A previous taxonomic analysis
262 (Daley et al., 2013a) suggested that this was potentially a *Hurdia* appendage. As the distal end of
263 the appendage is not preserved and the morphology of the ventral spines is not conclusive, it is
264 identified here as a hurdiid, but no identification to the genus level is made.
265
266 *Peytoia from the Marjum Formation*.—*Hurdia* is not known from the Marjum Formation. Briggs
267 and Robison (1984) identified USNM 374593 (Figs. 6, 7) from the Marjum Formation as a
268 partial body (lacking frontal appendages) of *Peytoia nathorsti*, based on the presence of
269 transverse lines on the flaps. These had only been observed in *P. nathorsti* and not
270 *Anomalocaris canadensis*, which at the time was the only other radiodontan body type known.
271 We support placement in *Peytoia* because of the presence of large posterior-tapering swim flaps
272 (in contrast to the small flaps of *Hurdia*) with transverse lines (which are absent in
273 *Anomalocaris*), and the absence of a tail fan (present in *Hurdia* and *Anomalocaris*). The
274 specimen consists of the 11 most posterior segments and tail of the animal, with flaps and central

body structures preserved together. There is slight overlap of the anterior and posterior edges of the flaps, and the presence of some high-relief mineralized structures (Fig. 7, described below). A dark brown-grey linear structure (‘ba’ in Fig. 6.5) runs down the median axis of the animal, 6–7 mm wide near the anterior, tapering to a point and disappearing as it reaches the pair of body flaps. This region has a very thin (1 mm wide) feature at its midline running along the length of the body, particularly visible in the counterpart (‘g’ in Fig. 6.5). This is interpreted to be the gut running through the body cavity. It is flanked on both sides by a series of bilaterally symmetrical dark grey features (‘s1–s11’ in Fig. 6.5). They are larger anteriorly (3 x 25 mm) than posteriorly (1.5 x 10 mm), and are interpreted as setal blade blocks on account of their preservation, position and co-occurrence with body flaps. Lateral to the setal blade structures, and partly overlapping them, there is a series of dark reflective structures with high relief, present in the region where the base of the flaps meets the axial region (‘m1–m6’ in Fig. 6.5). These structures are interpreted as musclulature on account of similarities between them and musculature in *Anomalocaris canadensis* (Daley and Edgecombe, 2014, figs. 15, 17). Both have a fibrous texture (Fig. 7.3–7.5) are similar in size and shape (Fig. 7) and are at the base of body flaps (Fig. 7.1, 7.2). In *A. canadensis* these structures are preserved as an orange material, or as a high relief dark grey to black reflective material. In *Peytoia* (USNM 374593) they are similarly preserved as high relief dark reflective material, although the fibrous details are less well preserved than in *A. canadensis* (compare Fig. 7.3, 7.5 to Fig. 7.4). They are not interpreted as gut diverticulae, which are often preserved as high relief dark reflective material, as they do not intersect the gut, and are instead associated with the intersection of the body flaps with the cuticularized body, far from the body axis. However it must be noted that euarthropod gut diverticulae are preserved in a variety of ways (Lerosey-Aubril et al., 2012), and the preservation of this musculature is

different from musculature reported from some other Burgess-Shale type localities: *Pambdelurion* from Sirius Passet (Budd, 1998); and *Myoscolex* from the Emu Bay Shale (Briggs and Nedin, 1997).

The second most anterior flap on the right side of the counterpart preserves a set of high-relief linear structures near its base, located between the musculature of this flap and the flap in front of it (Fig. 6.4, 'st' in Fig. 6.5). The six parallel, evenly spaced structures are mineralized, and although they are closely packed, they do not touch one another. The longest one, closest to the body axis, is just under 1 mm in length, and the structures become shorter away from the body axis, with the shortest one just under 0.5 mm in length. 2 mm below the linear structures there are a number of circular mineralized structures, around 0.25 to 0.5 mm in diameter. Small spheres 0.5 mm in diameter are present on other phosphatized blocks. Similar structures, which were identified as clusters of pyrite framboids, have been reported from the middle Cambrian (Series 3) Pioche Shale by Moore and Lieberman (2009). Transverse lines only cover the anterior portion of the flap (Fig. 6.3), and no internal structure of the flaps is preserved, similar to *P. nathorsti* from the Burgess Shale (Whittington and Briggs, 1985). Ten large ventral flaps ('vf1–vf10' in Fig. 6.5) are preserved on the side that most clearly shows a dorsal flap ('df1' in Fig. 6.5), and six large ventral flaps are preserved on the other side ('vf1–vf6' in Fig. 6.5), with one dorsal flap preserved there also ('df1' in Fig. 6.5). The front pair of flaps is the largest, and they reduce in size sequentially. The flaps associated with body segments 7–11 are overlapping due to the orientation of preservation. There are no flaps associated with the tail ('t' in Fig. 6.5). On the part, two dorsal flaps are also preserved at the front of the animal, in addition to the larger ventral flaps ('df1' in Fig. 6.5).

A partial mouthpart, KUMIP 314095 (Fig. 6.6, 6.7) is identified as *Peytoia* on account of

321 the visible plate morphology and lack of internal tooth rows. One large plate with large triangular
322 inner spines is preserved, with five smaller plates on one side and seven on the other side of the
323 large plate. These smaller plates are a regular size and overlap each other, with the plate closer to
324 the large plate overlapping the one next closest. The partially preserved central opening shows
325 no evidence of additional rows of teeth. The large plate has 10 small triangular spines pointing
326 inwards, the widest of which, at a central point of the plate, is around 2 mm. The others are
327 smaller, at around 1 mm wide. Some of the smaller plates have a single projection also pointing
328 inwards, around 1 mm wide. Unusually for *Peytoia* this mouthpart has small (diameter
329 approximately 0.3 mm) nodes on the surface of the large plate, and some adjacent plates (visible
330 on both part and counterpart, Fig. 6.6, 6.7).

331

332 **Discussion**

333

334 *Morphological interpretations on Hurdia appendages can be influenced by specimen*
335 *orientation*.—*Hurdia* appendages are preserved in a variety of orientations (see Daley et al.,
336 2013a). Ventral spines of *Hurdia* are often preserved curved, both anteriorly (e.g. Fig. 2.3, 2.4)
337 and posteriorly (e.g. Fig. 2.1, 2.2) and straight (e.g. Figs. 2.5, 3), sometimes in the same
338 specimen (e.g. Daley et al., 2009, fig. 2C). The appendages have some element of plasticity, and
339 during preservation they can become deformed. In some specimens the curvature of ventral
340 spines appears to change along the length of the appendage, due to the appendage being
341 preserved at an angle (e.g. Daley et al., 2013a, figs. 12C, E, 24A, where the distalmost ventral
342 spines appear more curved as the appendage is rotated one way, and Daley et al., 2013a, fig.
343 12G, where the proximalmost ventral spines appear more curved as the appendage is rotated the

344 other way). Appendages not preserved at such angles tend to have the distalmost podomeres
345 more clearly preserved, not overlapping more proximal podomeres (compare the position of the
346 distalmost podomeres in Fig. 3 and Daley et al., 2013a, fig. 12A, to those described as rotated
347 above).

348 The impact that these preservational factors might have on morphological reconstructions
349 and inferred evolutionary affinities can be observed by considering phylogenetic analyses of
350 Radiodonta. Recent phylogenies (Cong et al., 2014; Van Roy et al., 2015) based on the data
351 matrix and analysis of Vinther et al. (2014) consider four distinct representatives of *Hurdia*: *H.*
352 *victoria, H.* cf. *victoria* Utah*, H.* sp. B Spence Shale, and *H.* sp. B Burgess Shale (the latter two
353 were coded identically except for missing character states). Other than missing character states,
354 *H. victoria* and H. cf. *victoria* Utah only differ in the condition of character 29: Vinther et al.
355 (2014) coded *H. victoria* as having distally projecting dorsal spines on the terminal segments;
356 these were coded as absent in *Hurdia* cf. *victoria* Utah. Vinther et al. (2014) coded *Hurdia*
357 *victoria* (including *Hurdia* cf. *victoria* Utah) and *H.* sp. B as differing in three characters. In
358 character 34, the ventral spines were coded as broader distally than proximally in *Hurdia*
359 *victoria*, and subequal or narrower distally in *Hurdia* sp. B. In character 39, the distal tips of the
360 ventral spines are hooked forward in *Hurdia victoria*, but strongly hooked forward and forming a
361 90° angle with the spine base in *Hurdia* sp. B. The phylogenetic significance of characters 29,
362 34, and 39 may be called into question by the aforementioned preservational variation. Similarly,
363 character 46 (curvature of ventral spines) may reflect preservational rather than taxonomic
364 variation. *Hurdia* sp. B was coded as having proximal ventral spines that curve posteriorly,
365 whereas *H. victoria* was coded as having ventral spines all straight or anteriorly curved.
366 However, *H. victoria* specimens with straight proximal ventral spines and anteriorly curving

367 distal ends are common (e.g. Daley et al., 2013, fig. 12 A, C, E, G) and this reflects taphonomic
368 variation.

369 To visualize how the angle of preservation influences morphological interpretations of
370 *Hurdia* appendages, a 3D model was created in Blender based on the morphology of the *Hurdia*
371 appendage in Daley and Budd (2010, text-fig. 1D). This 3D model (Fig. 8) suggests that the
372 apparent broadness of ventral spines on distal podomeres will be influenced by how a specimen
373 is oriented when it is preserved, and so the broadness of ventral spines (Vinther et al., 2014,
374 Character 34) is likely not a good character for distinguishing *Hurdia* species. A small difference
375 in orientation affecting apparent thickness of ventral spines can be seen by comparing KUMIP
376 314086 (Fig. 5.1, 5.2, with ventral spines of equal thickness) and KUMIP 314042 (Fig. 2.5,
377 where the distalmost ventral spine appears thicker because of its orientation). This is visualized
378 by the 3D model, where Fig. 8.1 (no rotation) shows ventral spines of equal thickness, and Fig.
379 8.2 (small rotation) shows an apparently thicker distalmost ventral spine. A more extreme
380 example of the variation in the orientation of appendage preservation can be seen in the two
381 appendages of KUMIP 312405 (Fig. 3). These appendages are presumably from the same animal
382 but preserved at very different orientations.

383 In summary Vinther et al.'s (2014) characters 29, 34, 39, and 46, which comprise the
384 evidence to distinguish four different representatives of *Hurdia*, may be influenced by
385 preservational factors. A phylogenetic analysis of the data matrix from Van Roy et al. (2015),
386 which is based on the original data matrix of Vinther et al. (2014), was run in TNT v. 1.5 using
387 implicit enumeration under equal weighting. The data matrix was modified in the following
388 ways: In Character 29, *H.* cf. *victoria* Spence is coded as dorsal spines present, and both *H.* sp. B
389 taxa are coded as unknown; Character 34 was deleted as is has been shown to reflect

390 preservation and not true morphological difference; Character 39 (now Character 38) was
391 changed to being unordered, and both *H.* sp. B taxa and *Stanleycaris* were coded as having
392 hooked forward ventral spines; and in Character 46 (now Character 45), both *Hurdia* sp. B taxa
393 are coded as having straight or curved anterior ventral spines. An analysis under equal weighting
394 recovers 70 most parsimonious trees of 106 steps, and in strict consensus (CI=0.66, RI=0.85) all
395 four *Hurdia* taxa and *Stanleycaris* are recovered in an unresolved polytomy. This is in contrast to
396 the resolved relationships depicted in Vinther et al. (2014) and Van Roy et al. (2015), where the
397 two *H.* sp. B specimens form a clade that is sister to *Stanleycaris*, rather than to *H. victoria*.
398 Based on current evidence *Hurdia* cannot be identified to the species level by its frontal
399 appendages alone, and appendages from the Spence Shale and the Burgess Shale cannot be
400 distinguished as KUMIP 314040 and 314178, described herein, show that *Hurdia* appendages
401 from Utah do possess dorsal spines (Fig. 2.2–2.4). *Hurdia* can still only be separated into two
402 distinct species by the shape of its H-element (Daley et al., 2013a).
403
404 *Presence of nodes on mouthparts*.— Nodes are present on the plates of *Hurdia* mouthparts from
405 the Spence Shale (KUMIP 314175a/b and 314265a/b, Fig. 2.6, 2.7) and partial *Peytoia*
406 mouthparts from the Marjum Formation (KUMIP 314095, Fig. 6.6, 6.7). Nodes are not often
407 seen in Burgess Shale specimens. The nodes are similar to what is seen in *Anomalocaris* (e.g.,
408 Daley and Bergström, 2012, fig. 2a–d; Daley and Edgecombe, 2014, fig. 7.5). However, the
409 plates of these mouthparts lack the subdivisions and furrowing on the outer margins that is often
410 seen in *Anomalocaris* (e.g. Daley and Bergström, 2012, fig. 2g–j). The presence of nodes in the
411 Utah specimens could be due to interspecific variation, however, a more likely cause is
412 preservational differences, which allow more 3D structure to be preserved in Utah than in

Burgess Shale specimens. Similar preservational differences are seen in the oral cones of *A. canadensis*, where nodes are preserved in varying degrees of relief in oral cones from the Burgess Shale and the Emu Bay Shale (Daley et al., 2013b, Daley and Bergström, 2012).

Geographical and temporal distribution of hurdiids.—*Hurdia* and *Peytoia* are distributed over a large temporal and geographic range (Table 2). Both are reported from China, the USA, and Canada. *Hurdia* is known additionally from the Czech Republic (Chlupáč and Kordule, 2002), and *Peytoia* from Poland (Daley and Legg, 2015). This study shows that *Peytoia* is not known from the Spence Shale. This does not have any implications for the first or last appearance of *Peytoia*, as its oldest occurrence is from Holy Cross Mountains (Daley and Legg, 2015) and it is reported from the younger Marjum Formation (Briggs and Robison, 1984, this study), however it does change the earliest known occurrence of *P. nathorsti* to the Burgess Shale. *Hurdia* is not yet known from the Marjum Formation, however it is reported from the younger Fezouata Lagerstätten (Van Roy and Briggs, 2011). As *Hurdia* and *Peytoia* do not co-occur in the Spence Shale or Marjum Formations, a potential hypothesis is that the similarities of their frontal appendages, and hence similar predation methods prevented the two genera from co-existing. Indeed, a recent morphospace analysis of the first appendages of 36 euarthropod taxa (Aria and Caron, 2015) supports functional similarities in the feeding appendages of *Peytoia* and *Hurdia*, which plotted close together. However, *Hurdia* and *Peytoia* do co-occur in the Wheeler Formation, Tulip Beds and Burgess Shale (Table 2), suggesting that they were capable of co-existing in the right environment, and the collection of more hurdiids from the Spence Shale and Marjum Formation may in fact show that *Peytoia* and *Hurdia* are present where currently they are not known.

Acknowledgments

M. Florence provided access to the specimen at the USNM. We thank the editor Jisuo Jin, Associate Editor Z. Zhang, an anonymous reviewer and J. Ortega-Hernandez for their valuable comments, and P. Selden (University of Kansas) for use of photographic equipment. The program TNT was made available with the sponsorship of the Willi Hennig Society. Funding was provided by a Palaeontological Association Sylvester-Bradley Award (PA-SB201503) to SP, the OUMNH to ACD and NSF-EAR-0518976 to BSL.

References

Aria, C., and Caron, J.B., 2015, Cephalic and limb anatomy of a new isoxyid from the burgess shale and the role of "stem bivalved arthropods" in the disparity of the frontalmost appendage: PloS one, v. 10, p. e0124979.

Babcock, L.E., and Robison, R.A., 1988, Taxonomy and paleobiology of some Middle Cambrian *Scenella* (Cnidaria) and hyolithids (Mollusca) from western North America: University of Kansas Paleontological Contributions, v. 121, p. 1–22.

Brett, C.E., Allison, P.A., DeSantis, M.K., Liddell, W.D., and Kramer, A., 2009, Sequence stratigraphy, cyclic facies, and lagerstätten in the Middle Cambrian Wheeler and Marjum formations, Great Basin, Utah: Palaeogeography, Palaeoclimatology, Palaeoecology, v. 277, p. 9–33.

Briggs, D.E., and Nedin, C., 1997, The taphonomy and affinities of the problematic fossil *Myoscolex* from the Lower Cambrian Emu Bay Shale of South Australia: Journal of Paleontology, v. 71, p.22–32.

Briggs, D.E., and Robison, R.A., 1984, Exceptionally preserved nontrilobite arthropods and *Anomalocaris* from the Middle Cambrian of Utah: University of Kansas Paleontological Contributions, v. 111, p. 1–23.

Briggs, D.E., Lieberman, B.S., Halgedahl, S.L. and Jarrard, R.D., 2005, A new metazoan from the Middle Cambrian of Utah and the nature of the Vetulicolia: Palaeontology, v. 48, p. 681–686.

Briggs, D.E., Lieberman, B.S., Hendricks, J.R., Halgedahl, S.L. and Jarrard, R.D., 2008, Middle Cambrian arthropods from Utah: Journal of Paleontology, v. 82, p. 238–254.

Brooks, H.K., and Caster, K.E., 1956, *Pseudoarctolepis sharpi*, n. gen., n. sp.(Phyllocarida), from the Wheeler Shale (Middle Cambrian) of Utah: Journal of Paleontology, v. 30, p. 9–14.

Bruton, D.L., 1981, The arthropod *Sidneyia inexpectans*, Middle Cambrian, Burgess Shale, British Columbia: Philosophical Transactions of the Royal Society of London. Series B, Biological Sciences, v. 295, p. 619–653.

Budd, G.E., 1998, Stem group arthropods from the Lower Cambrian Sirius Passet fauna of north Greenland, *in* Fortey, R. A., and Thomas, R. H., ed., Arthropod relationships, p. 125-138. Springer Netherlands.

Caron, J.B., Gaines, R.R., Mángano, M.G., Streng, M., and Daley, A.C., 2010, A new Burgess Shale–type assemblage from the "thin" Stephen Formation of the southern Canadian Rockies: Geology, v. 38, p. 811–814.

Chen, J.Y., Ramsköld, L., and Zhou, G.Q., 1994, Evidence for monophyly and arthropod affinity of Cambrian giant predators: Science, v. 264, p. 1304–1308.

Chlupáč, I., and Kordule, V., 2002, Arthropods of Burgess Shale type from the Middle Cambrian of Bohemia (Czech Republic): Bulletin of the Czech Geological Survey, v. 77, p. 167–182.

Cong, P., Ma, X., Hou, X., Edgecombe, G.D., Strausfeld, N.J., 2014, Brain structure resolves the segmental affinity of anomalocaridid appendages: Nature, v. 513, p. 538-542.

Conway Morris, S., and Robison, R.A., 1982, The enigmatic medusoid *Peytoia* and a comparison of some Cambrian biotas: Journal of Paleontology, v. 56, p. 116–122.

Conway Morris, S., and Robison, R.A., 1986., Middle Cambrian priapulids and other soft-bodied fossils from Utah and Spain: University of Kansas Paleontological Contributions, v. 117, p. 1–22.

Conway Morris, S., and Robison, R.A., 1988, More soft-bodied animals and algae from the Middle Cambrian of Utah and British Columbia: University of Kansas Paleontological Contributions, v. 122, p. 1–48

Conway Morris, S., Selden, P.A., Gunther, G., Jamison, P.G. and Robison, R.A., 2015, New records of Burgess Shale-type taxa from the middle Cambrian of Utah: Journal of Paleontology, v. 89, p. 411–423.

Cui, Z., and Huo, S.,1990, New discoveries of Lower Cambrian crustacean fossils from Western Hubei: Acta Palaeontologica Sinica, v. 29, p. 321–330.

Daley, A.C., and Bergström, J., 2012, The oral cone of *Anomalocaris* is not a classic ‘‘*Peytoia*’’: Naturwissenschaften, v. 99, p. 501–504.

Daley, A.C., and Budd, G.E., 2010, New anomalocaridid appendages from the Burgess Shale, Canada: Palaeontology, v. 53, p. 721–738.

Daley, A.C., and Edgecombe, G.D., 2014, Morphology of *Anomalocaris canadensis* from the Burgess Shale: Journal of Paleontology, v. 88, p. 68–91.

Daley, A.C., and Legg, D.A., 2015, A morphological and taxonomic appraisal of the oldest anomalocaridid from the Lower Cambrian of Poland: Geological Magazine, v. 152, p. 949–955.

Daley, A.C., Budd, G.E., Caron, J.B., Edgecombe, G.D. and Collins, D., 2009, The Burgess Shale anomalocaridid *Hurdia* and its significance for early euarthropod evolution: Science, v. 323, p. 1597–1600.

Daley, A.C., Budd, G.E. and Caron, J.B., 2013a, Morphology and systematics of the anomalocaridid arthropod *Hurdia* from the Middle Cambrian of British Columbia and Utah: Journal of Systematic Palaeontology, v. 11, p. 743–787.

Daley, A.C., Paterson, J.R., Edgecombe, G.D., García-Bellido, D.C. and Jago, J.B., 2013b, New anatomical information on *Anomalocaris* from the Cambrian Emu Bay Shale of South Australia and a reassessment of its inferred predatory habits: Palaeontology, v. 56, p. 971–990.

Elrick, M., and Snider, A.C., 2002, Deep-water stratigraphic cyclicity and carbonate mud mound development in the Middle Cambrian Marjum Formation, House Range, Utah, USA: Sedimentology, v. 49, p. 1021–1047.

Gaines, R.R., 2014, Burgess Shale-type preservation and its distribution in space and time. Reading and Writing of the Fossil Record: Preservational Pathways to Exceptional Fossilization: Paleontological Society Papers, v. 20, p. 123–146.

Gaines, R.R., and Droser, M.L., 2003, Paleoecology of the familiar trilobite *Elrathia kingii*: An early exaerobic zone inhabitant: Geology, v. 31, p. 941–944.

Gaines, R.R., and Droser, M.L., 2005, New approaches to understanding the mechanics of Burgess Shale-type deposits: from the micron scale to the global picture: Sedimentary Record v. 3, p. 4–8.

Gaines, R.R., and Droser, M.L., 2010, The paleoredox setting of Burgess Shale-type deposits: Palaeogeography, Palaeoclimatology, Palaeoecology, v. 297, p. 649–661.

Gaines, R.R., Briggs, D.E., and Yuanlong, Z., 2008, Cambrian Burgess Shale–type deposits share a common mode of fossilization: Geology, v. 36, p. 755–758.

Gaines, R.R., Kennedy, M.J., and Droser, M.L., 2005, A new hypothesis for organic preservation of Burgess Shale taxa in the middle Cambrian Wheeler Formation, House Range, Utah: Palaeogeography, Palaeoclimatology, Palaeoecology, v. 220, p. 193–205.

Garson, D.E., Gaines, R.R., Droser, M.L., Liddell, W.D. and Sappenfield, A., 2012, Dynamic palaeoredox and exceptional preservation in the Cambrian Spence Shale of Utah: Lethaia, v. 45, p. 164–177.

Goloboff, P., and Catalano, S., 2016, TNT version 1.5, including a full implementation of phylogenetic morphometrics: Cladistics, v. 32, p. 221-238.

Gunther, L. F., and Gunther, V. G., 1981, Some Middle Cambrian fossils of Utah: Brigham Young University Geology Studies, v. 28, p. 1–81.

Halgedahl, S.L., Jarrard, R.D., Brett, C.E., and Allison, P.A., 2009, Geophysical and geological signatures of relative sea level change in the upper Wheeler Formation, Drum Mountains, West-Central Utah: a perspective into exceptional preservation of fossils: Palaeogeography, Palaeoclimatology, Palaeoecology, v. 277, p. 34–56.

Hendricks, J.R., 2013, Global distributional dynamics of Cambrian clades as revealed by Burgess Shale-type deposits: Geological Society, London, Memoirs, v. 38, p. 35–43.

Hendricks, J.R., and Lieberman, B.S., 2008, New phylogenetic insights into the Cambrian radiation of arachnomorph arthropods: Journal of Paleontology, v. 82, p. 585–594.

Hendricks, J.R., Lieberman, B.S. and Stigall, A.L., 2008, Using GIS to study palaeobiogeographic and macroevolutionary patterns in soft-bodied Cambrian arthropods: Palaeogeography, Palaeoclimatology, Palaeoecology, v. 264, p. 163–175.

Hou, X., Bergström, J. and Ahlberg, P., 1995, *Anomalocaris* and other large animals in the Lower Cambrian Chengjiang fauna of southwest China: GFF, v. 117, p. 163–183.

Johnston, P.A., Johnston, K.J., Collom, C.J., Powell, W.G. and Pollock, R.J., 2009, Palaeontology and depositional environments of ancient brine seeps in the Middle Cambrian Burgess Shale at The Monarch, British Columbia, Canada: Palaeogeography, Palaeoclimatology, Palaeoecology, v. 277, p. 86–105.

Kloss, T.J., Dornbos, S.Q., Chen, J.Y., McHenry, L.J., and Marenco, P.J., 2015, High-resolution geochemical evidence for oxic bottom waters in three Cambrian Burgess Shale-type deposits: Palaeogeography, Palaeoclimatology, Palaeoecology, v. 440, p. 90–95.

Lerosey-Aubril, R., Hegna, T.A., Kier, C., Bonino, E., Habersetzer, J., and Carré, M., 2012, Controls on gut phosphatisation: the trilobites from the Weeks Formation Lagerstätte (Cambrian; Utah): PLoS One, v7, p. e32934.

Lerosey-Aubril, R., Hegna, T.A., Babcock, L.E., Bonino, E., and Kier, C., 2014, Arthropod appendages from the Weeks Formation Konservat-Lagerstätte: new occurrences of anomalocaridids in the Cambrian of Utah, USA: Bulletin of Geosciences, v. 89, p. 269–282.

Liddell, W.D., Wright, S.W. and Brett, C.E., 1997, Sequence stratigraphy and paleoecology of the Middle Cambrian Spence Shale in northern Utah and southern Idaho: Brigham Young University Geology Studies, v. 42, p. 59–78.

LoDuca, S.T., Caron, J.B., Schiffbauer, J.D., Xiao, S., and Kramer, A., 2015, A reexamination of Yuknessia from the Cambrian of British Columbia and Utah: Journal of Paleontology, v. 89, p. 82–95.

Liu, Q., 2013, The first discovery of anomalocaridid appendages from the Balang Formation (Cambrian Series 2) in Hunan, China: Alcheringa, v. 37, p. 1–6.

Maddison, W.P., and Maddison, D.R., 2017, Mesquite: a modular system for evolutionary analysis. Version 3.2: http://mesquiteproject.org.

Moore, R.A., Lieberman, B.S., 2009, Preservation of early and Middle Cambrian soft-bodied arthropods from the Pioche Shale, Nevada, USA: Palaeogeography, Palaeoclimatology, Palaeoecology, v. 277, p. 57–62.

Olcott Marshall, A., Wehrbein, R.L., Lieberman, B.S. and Marshall, C.P., 2012, Raman spectroscopic investigations of Burgess Shale–type preservation: a new way forward: Palaios, v. 27, p. 288–292.

Rees, M.N., 1986, A fault-controlled trough through a carbonate platform: The Middle Cambrian House Range embayment: Geological Society of America Bulletin, v. 97, p. 1054–1069.

Resser, C.E., 1939, The Spence shale and its fauna, (with six plates): Smithsonian Institution Miscellaneous Collections, v. 97, p. 1–29.

Robison, R.A., 1964, Late Middle Cambrian faunas from western Utah: Journal of Paleontology, v. 38, p. 510–566.

Robison, R. A. 1965, Middle Cambrian eocrinoids from western North America: Journal of Paleontology, v. 39, p. 355–364.

Robison, R.A., 1991, Middle Cambrian biotic diversity: examples from four Utah Lagerstätten, in Simonetta, A. and Conway Morris, S., ed, The early evolution of metazoa and the significance of problematic taxa: Cambridge University Press, Cambridge, p.77–98.

Robison, R.A. and Babcock, L.E., 2011, Systematics, paleobiology, and taphonomy of some exceptionally preserved trilobites from Cambrian Lagerstätten of Utah: Paleontological contributions, v. 5, p. 1–47.

Robison, R.A. and Richards, B.C., 1981, Larger bivalve arthropods from the Middle Cambrian of Utah: University of Kansas Paleontological Contributions, v. 106, p. 1–28

Robison, R.A. and Wiley, E.O., 1995, A new arthropod, *Meristosoma*: more fallout from the Cambrian explosion: Journal of Paleontology, v. 69, p. 447–459.

Robison, R.A., Babcock, L.E., and Gunther, V.G., 2015, Exceptional Cambrian fossils from Utah: a window into the Age of Trilobites: Utah Geological Survey Miscellaneous Publications, v. 15, p. 1–97.

Rogers, J.C., 1984, Depositional environments and paleoecology of two quarry sites in the Middle Cambrian Marjum and Wheeler Formations, House Range, Utah: Brigham Young University Geology Studies, v. 31, p. 97–115.

Stein, M., 2013, Cephalic and appendage morphology of the Cambrian arthropod *Sidneyia inexpectans*: Zoologischer Anzeiger–A Journal of Comparative Zoology, v. 253, p. 164–178.

Stein, M., Church, S.B., and Robison, R.A., 2011, A new Cambrian arthropod, *Emeraldella brutoni*, from Utah: Paleontological Contributions, v. 3, p.1–9.

Van Roy, P., and Briggs, D.E., 2011, A giant Ordovician anomalocaridid: Nature, v. 473, p.510–513.

Van Roy, P., Daley, A.C., and Briggs, D.E.G., 2015, Anomalocaridid trunk limb homology revealed by a giant filter-feeder with paired flaps. Nature, v. 522, p. 77-80.

Vinther, J., Stein, M., Longrich, N.R., and Harper, D.A., 2014, A suspension-feeding anomalocarid from the Early Cambrian: Nature, v. 507, p. 496–499.

Walcott, C. D., 1911, Middle Cambrian holothurians and medusa: Smithsonian Miscellaneous Collections, v. 57, p. 41-68.

Walcott, C. D., 1912, Middle Cambrian Brachiopoda, Malacostraca, Trilobita and Merostomata: Smithsonian Miscellaneous Collections, v. 57, p. 145–288.

Whiteaves, J. F., 1892, Description of a new genus and species of phyllocarid Crustacea from the Middle Cambrian of Mount Stephen, B.C.: Canadian Record of Science, v. 5, p. 205–208.

Whittington, H.B., and Briggs, D.E., 1985, The largest Cambrian animal, *Anomalocaris*, Burgess Shale, British Columbia: Philosophical Transactions of the Royal Society of London. Series B, Biological Sciences, v. 309, p.569–609.

Figure captions

Figure 1. Stratigraphic column showing relative ages of Burgess Shale, Spence Shale, Wheeler Formation, Marjum Formation and Weeks Formation, with reference to global chronostratigraphic units and polymerid trilobite biostratigraphy. Adapted from Robison et al. (2015).

Figure 2. Hurdiid appendages and oral cones from the Spence Shale Member, Langston Formation, Wellsville Mountains, Utah, USA. **(1)** Appendage KUMIP 314145; **(2)** appendage KUMIP 314178; **(3)** appendage KUMIP 314040a with arrow indicating broken ventral spine; **(4)** KUMIP 314040b, counterpart to **3**; **(5)** appendage KUMIP 314042; **(6)** oral cone KUMIP 314175a; **(7)** oral cone KUMIP 314265a; All scale bars represent 5 mm.

Figure 3. Assemblage of two *Hurdia* appendages with an oral cone **(1)** KUMIP 312405a; **(2)** KUMIP 312405b, counterpart to **1**; **(3)** interpretative drawing of **2**. Abbreviations: app. 1 = appendage 1, app. 2 = appendage 2, as = auxiliary spine, lp = large plate, p1 = podomere 1, p6 = podomere 6, tr = tooth row, ts = terminal spine, vs = ventral spine. All scale bars represent 10 mm.

Figure 4. *Hurdia* carapace elements and flap from the Spence Shale Member, Langston Formation, Wellsville Mountains, Utah, USA. **(1)** H-element KUMIP 314050; **(2)** H-element KUMIP 314039; **(3)** H-element 314058; **(4)** Boxed region in **1**; **(5)** Boxed region in **3**; **(6)** flap KUMIP 314057b; **(7)** KUMIP 314057a, part to **6**. Scale bars in **1**–**3**, **6, 7** represent 10 mm, scale bars in **4, 5** represent 2.5 mm.

Figure 5. Hurdiid appendages, oral cones and carapace element from the Wheeler Formation, House Range, Utah, USA. **(1)** Appendage KUMIP 314086b; **(2)** KUMIP 314086a, part to **1**; **(3)** appendage KUMIP 204781a; **(4)** KUMIP 204781b, counterpart to **3**; **(5)** oral cone KUMIP 314094; **(6)** *Hurdia* P-element 153901a; **(7)** KUMIP 153901b, counterpart to **6**; **(8)** oral cone

KUMIP 314078b; **(9)** KUMIP 314078a, part to **8**; **(10)** oral cone KUMIP 153093b; **(11)** KUMIP 153093a, part to **10**. All scale bars represent 10 mm.

Figure 6. *Peytoia* partial body and partial oral cone from the Marjum Formation, House Range, Utah, USA, USNM 374593 **(1)** Counterpart; **(2)** part; **(3)** box from **1**, showing flap and strengthening rays; **(4)** box from **2**, arrow indicates high relief linear structures; **(5)** interpretive sketch of **1**. Abbreviations: ba = body axis, s1–11 = setal blade blocks, labelled anterior to posterior, df = dorsal flap, g = gut, hr? = head region?, m1–6 = muscle blocks, labelled anterior to posterior, st = staples, t = tail, vf = ventral flap; **(6)** partial oral cone KUMIP 314095b; **(7)** part to **6**; All scale bars represent 10 mm.

Figure 7. Comparison of musculature in *Peytoia* partial body from the Marjum Formation, House Range, Utah, USA, and *Anomalocaris* from the Burgess Shale, British Columbia, Canada. **(1)** USNM 374593, box **7.1** from Fig. 6.1, showing position of musculature at the base of flaps; **(2)** ROM 62547, showing position of musculature at the base of flaps; **(3)** box from **1**, showing faint linear features in musculature; **(4)** box from **2**, showing clear linear features in musculature **(5)** box **7.5** from Fig. 6.1, showing linear features in matrix where musculature has been removed. Scale bars in **1, 2,** represent 10 mm. Scale bars in **3, 4, 5** represent 1 mm.

Figure 8. 3D model of *Hurdia* appendage, with ventral spines reconstructed as being of equal thickness. **(1)** Lateral view, showing ventral spines appearing equally thick; **(2)** oblique view,

showing distal ventral spines appearing thicker than proximal ones, and differences in 'hooked' appearance at distal tip of ventral spines.

Table captions

Table 1. Specimens examined in this study, including original and new taxonomic interpretations.

Table 2. Locations containing hurdiid specimens. Abbreviations: HCM = Holy Cross Mountains, Poland; Shuj. = Shuijingtuo Formation, China; Balang = Balang Formation, China; Jince = Jince Formation, Czech Republic; Spence = Langston Formation (Spence Shale Member), Utah, USA; Tulip = Tulip Beds, Mount Stephen, Yoho National Park, Canada; Burg. = Fossil Ridge, Burgess Shale, Yoho National Park Canada; Stan. = Stanley Glacier, Kootenay National Park, Canada; Wheel. = Wheeler Formation, Utah, USA; Marj. = Marjum Formation, Utah, USA; Fez. = Fezouata Formation, Morocco. Publications: 1=Daley and Legg (2015); 2=Cui and Hou (1990); 3=Lui (2013); 4= Chlupáč and Kordule (2002); 5=Conway Morris and Robison (1988); 6=Briggs et al. (2008); 7=Daley and Budd (2010); 8=Caron et al. (2010); 9=Robison and Richards (1981); 10=Briggs and Robison (1984); 11=Van Roy and Briggs (2011).

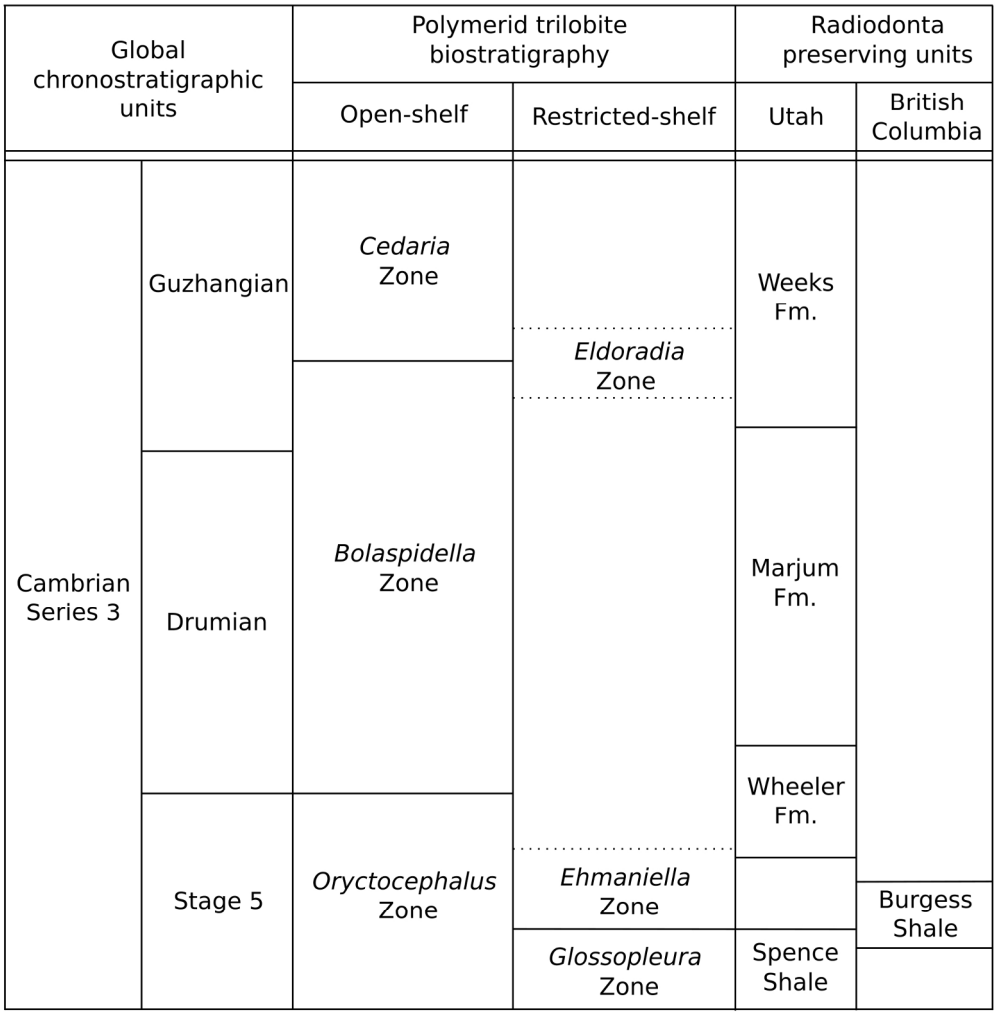

Stratigraphic column showing relative ages of Burgess Shale, Spence Shale, Wheeler Formation, Marjum Formation and Weeks Formation, with reference to global chronostratigraphic units and polymerid trilobite biostratigraphy. Adapted from Robison et al. (2015).

Figure 1

180x182mm (300 x 300 DPI)

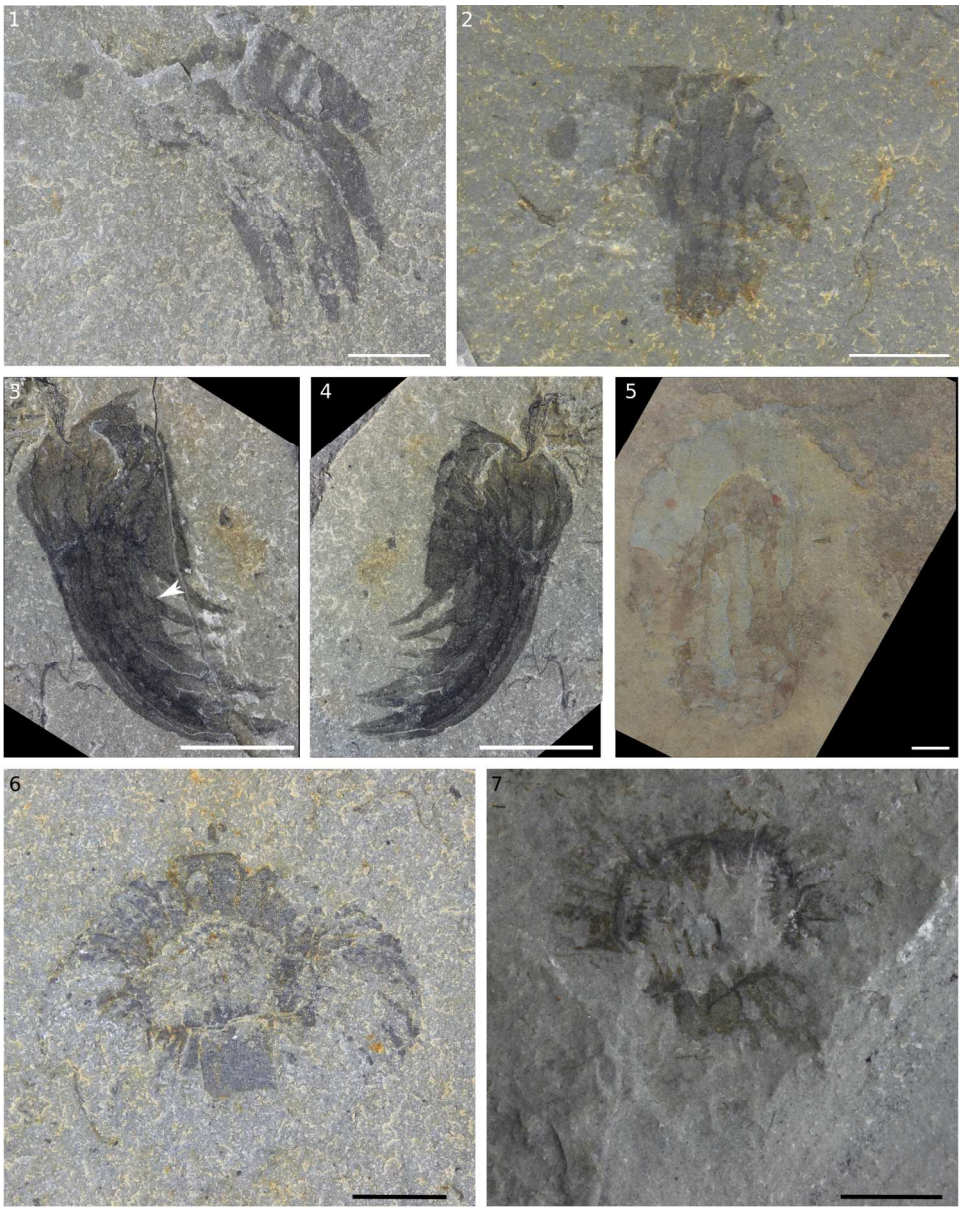

Hurdiid appendages and oral cones from the Spence Shale Member, Langston Formation, Wellsville Mountains, Utah, USA. (1) Appendage KUMIP 314145; (2) appendage KUMIP 314178; (3) appendage KUMIP 314040a with arrow indicating broken ventral spine; (4) KUMIP 314040b, counterpart to 3; (5) appendage KUMIP 314042; (6) oral cone KUMIP 314175a; (7) oral cone KUMIP 314265a; All scale bars represent 5 mm.

Figure 2
170x214mm (300 x 300 DPI)

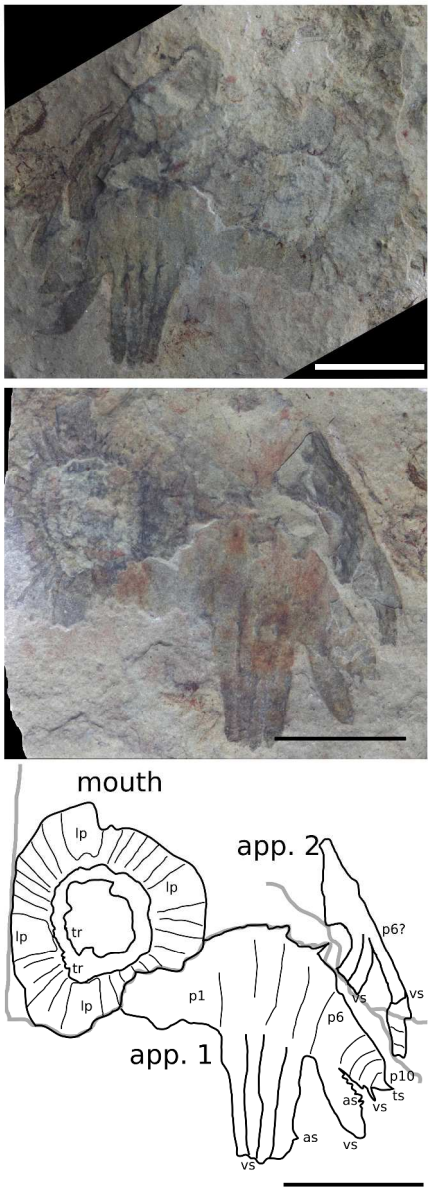

Assemblage of two Hurdia appendages with an oral cone (1) KUMIP 312405a; (2) KUMIP 312405b, counterpart to 1; (3) interpretative drawing of 2. Abbreviations: app. 1 = appendage 1, app. 2 = appendage 2, as = auxiliary spine, lp = large plate, p1 = podomere 1, p6 = podomere 6, tr = tooth row, ts = terminal spine, vs = ventral spine. All scale bars represent 10 mm.

Figure 3
242x670mm (600 x 600 DPI)

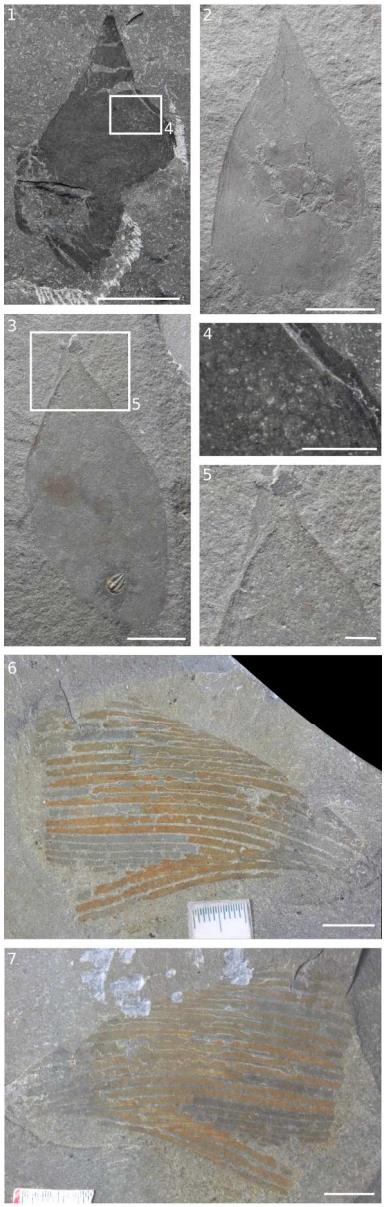

Hurdia carapace elements and flap from the Spence Shale Member, Langston Formation, Wellsville Mountains, Utah, USA. (1) H-element KUMIP 314050; (2) H-element KUMIP 314039; (3) H-element 314058; (4) Boxed region in 1; (5) Boxed region in 3; (6) flap KUMIP 314057b; (7) KUMIP 314057a, part to 6. Scale bars in 1–3, 6, 7 represent 10 mm, scale bars in 4, 5 represent 2.5 mm.

Figure 4
85x270mm (300 x 300 DPI)

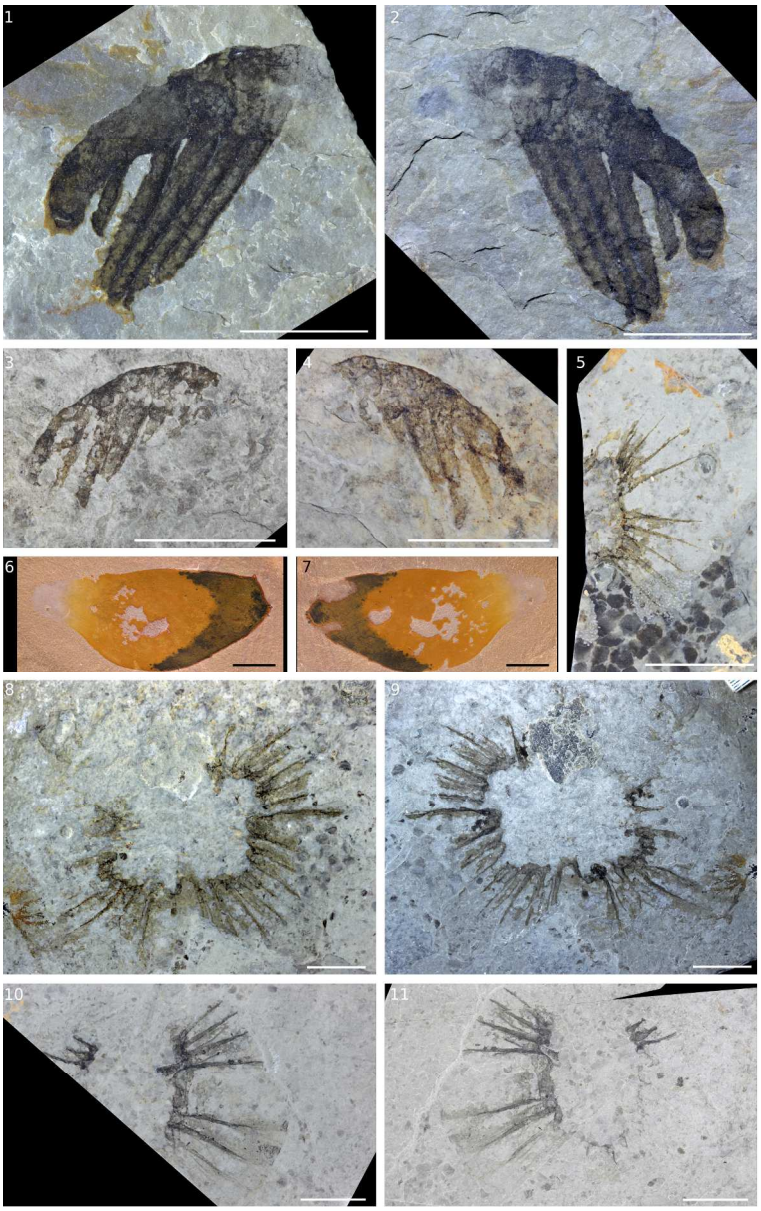

Hurdiid appendages, oral cones and carapace element from the Wheeler Formation, House Range, Utah, USA. (1) Appendage KUMIP 314086b; (2) KUMIP 314086a, part to 1; (3) appendage KUMIP 204781a; (4) KUMIP 204781b, counterpart to 3; (5) oral cone KUMIP 314094; (6) Hurdia P-element 153901a; (7) KUMIP 153901b, counterpart to 6; (8) oral cone KUMIP 314078b; (9) KUMIP 314078a, part to 8; (10) oral cone KUMIP 153093b; (11) KUMIP 153093a, part to 10. All scale bars represent 10 mm.

Figure 5
170x270mm (300 x 300 DPI)

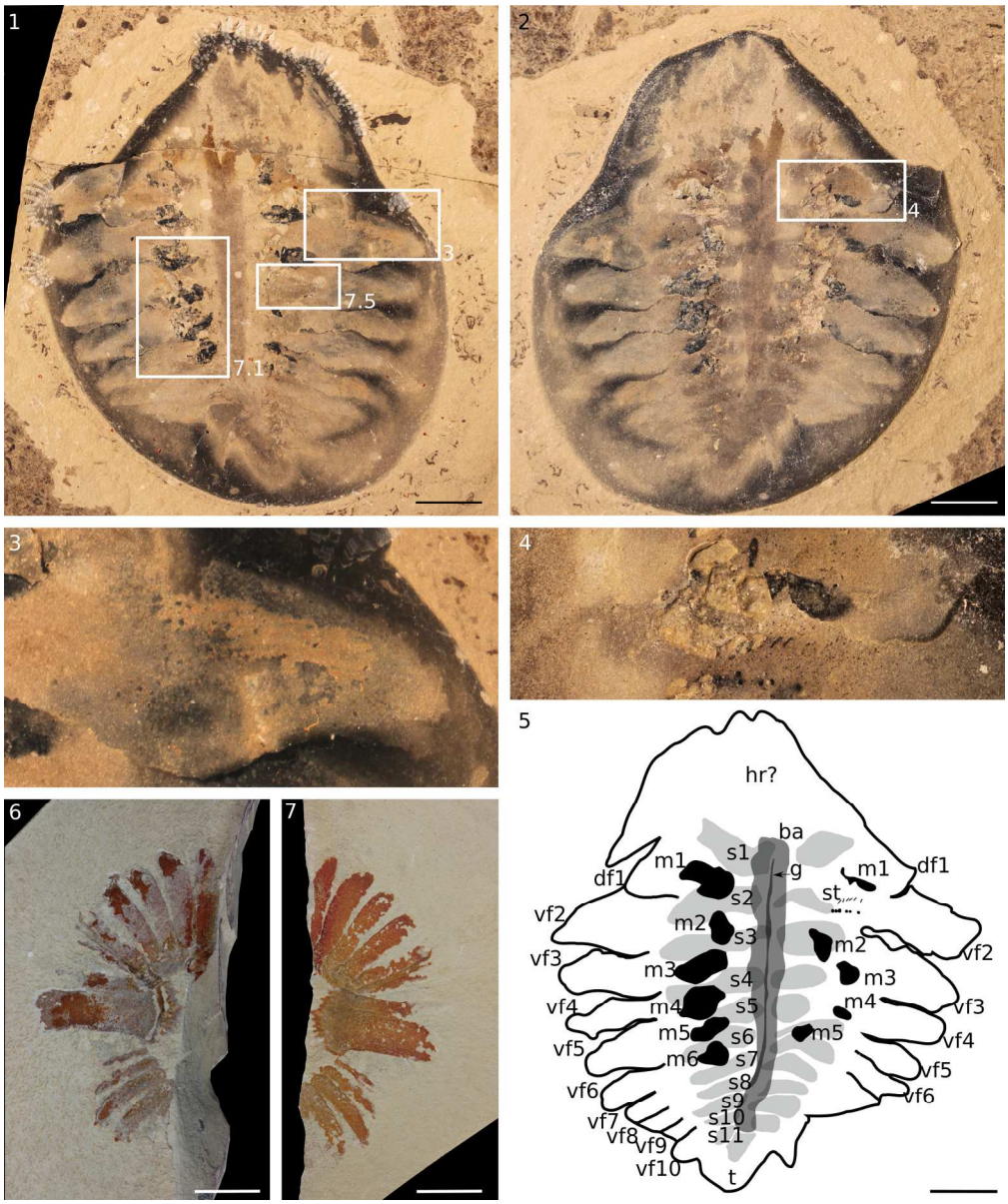

Peytoia partial body and partial oral cone from the Marjum Formation, House Range, Utah, USA, USNM 374593 (1) Counterpart; (2) part; (3) box from 1, showing flap and strengthening rays; (4) box from 2, arrow indicates high relief linear structures; (5) interpretive sketch of 1. Abbreviations: ba = body axis, s1–11 = setal blade blocks, labelled anterior to posterior, df = dorsal flap, g = gut, hr? = head region?, m1–6 = muscle blocks, labelled anterior to posterior, st = staples, t = tail, vf = ventral flap; (6) partial oral cone KUMIP 314095b; (7) part to 6; All scale bars represent 10 mm.

Figure 6
170x202mm (300 x 300 DPI)

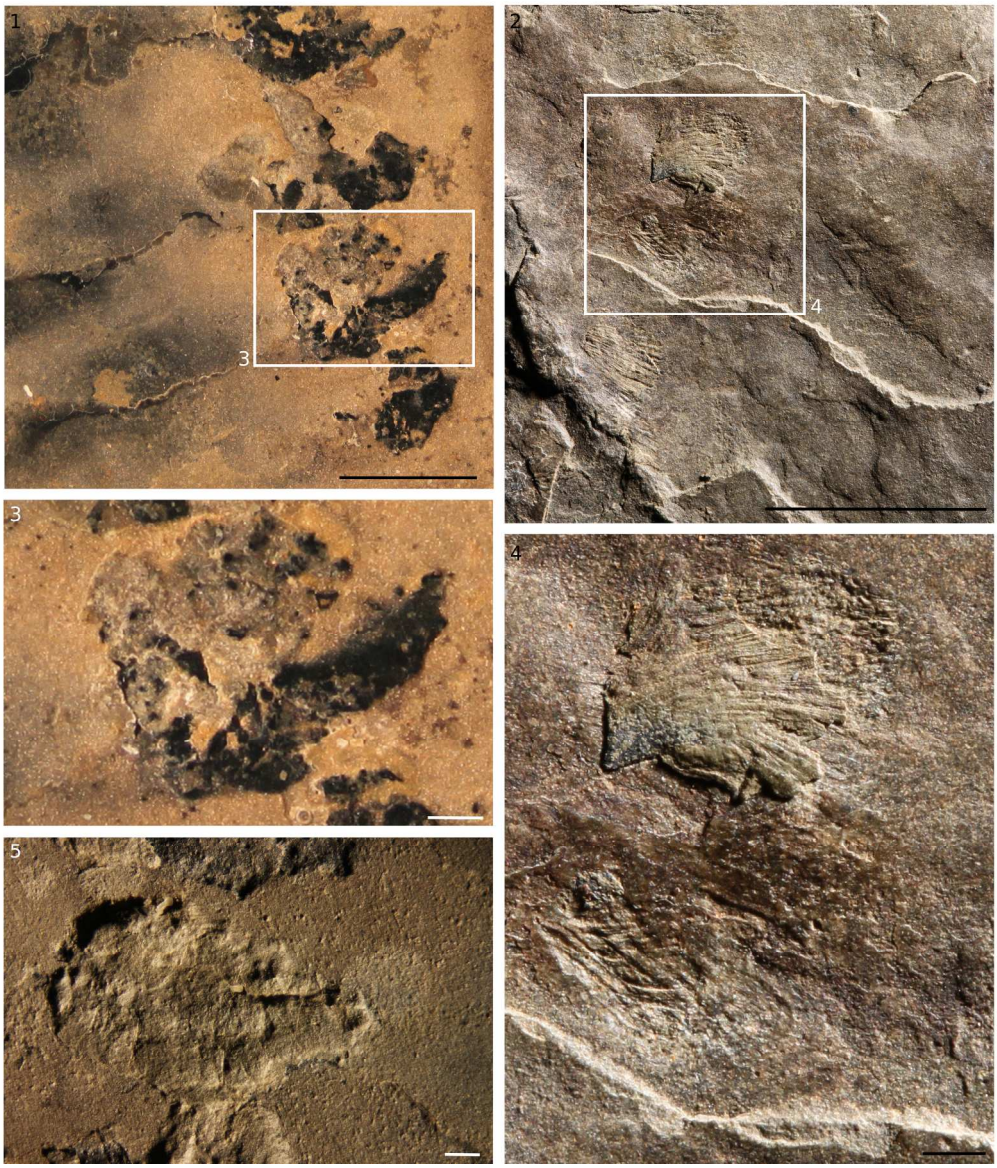

Comparison of musculature in Peytoia partial body from the Marjum Formation, House Range, Utah, USA, and Anomalocaris from the Burgess Shale, British Columbia, Canada. (1) USNM 374593, box 7.1 from Fig. 6.1, showing position of musculature at the base of flaps; (2) ROM 62547, showing position of musculature at the base of flaps; (3) box from 1, showing faint linear features in musculature; (4) box from 2, showing clear linear features in musculature (5) box 7.5 from Fig. 6.1, showing linear features in matrix where musculature has been removed. Scale bars in 1, 2, represent 10 mm. Scale bars in 3, 4, 5 represent 1 mm.

Figure 7
209x245mm (300 x 300 DPI)

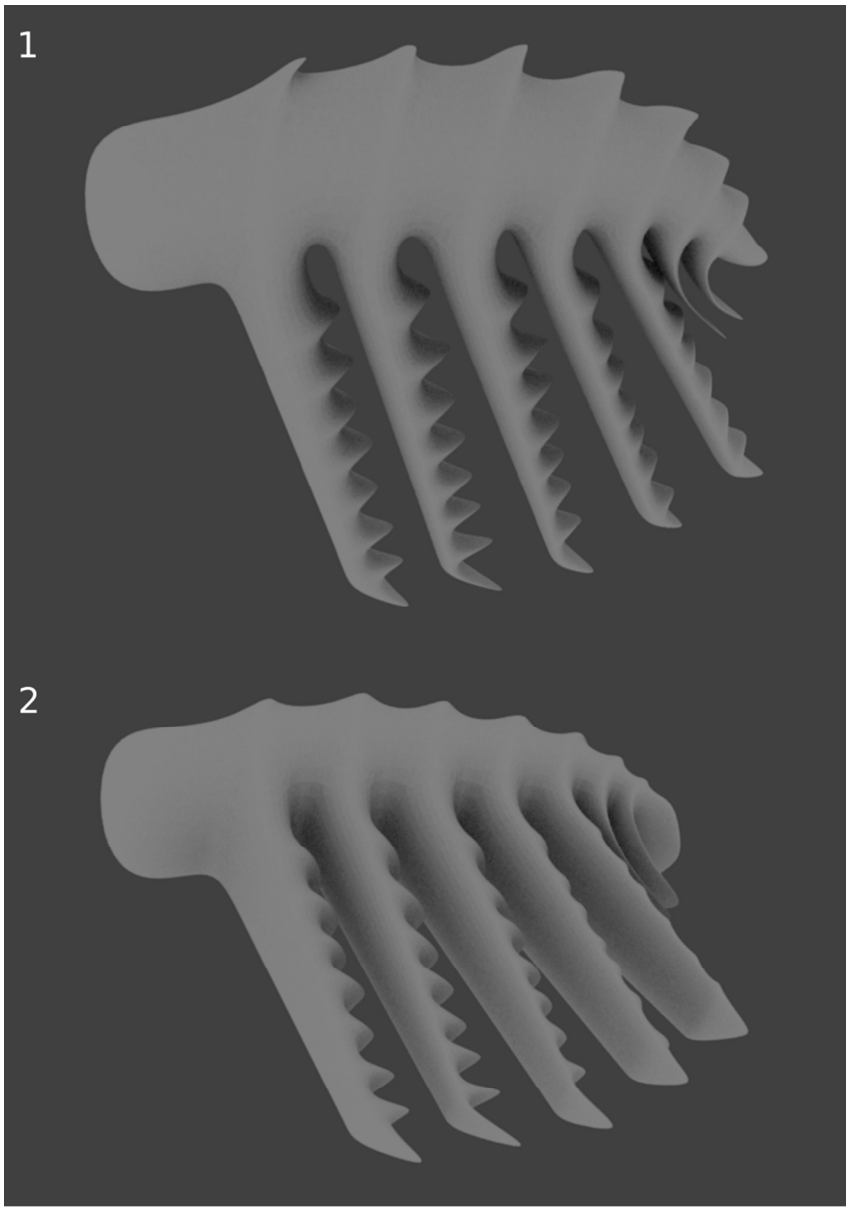

. 3D model of Hurdia appendage, with ventral spines reconstructed as being of equal thickness. (1) Lateral view, showing ventral spines appearing equally thick; (2) oblique view, showing distal ventral spines appearing thicker than proximal ones, and differences in 'hooked' appearance at distal tip of ventral spines.

Figure 8
85x121mm (300 x 300 DPI)

Catalogue number	Figure	Locality Age	Previous interpretation	Reference	New interpretation	Fragment
KUMIP 153093a/b	5.10, 5.11	Wheeler Formation Cambrian Drumian	*Peytoia* cf. *nathorsti*	Conway Morris & Robison, 1982	*Peytoia nathorsti*	Mouthpart
KUMIP 153094	5.5	Wheeler Formation Cambrian Drumian	*Peytoia* cf. *nathorsti*	Conway Morris & Robison, 1982	*Peytoia nathorsti*	Mouthpart
KUMIP 153901a/b	5.6, 5.7	Wheeler Formation, Cambrian Drumian	*Proboscocaris agnosta* *Hurdia*	Robison & Richards, 1981; Daley et al., 2013a	*Hurdia*	P-element
KUMIP 204777-204780	Conway Morris and Robison, 1988, figs. 26.1a, 26.1b, 26.2	Spence Shale Cambrian Stage 5	*Peytoia* cf. *nathorsti*	Conway Morris & Robison, 1988	*Sidneyia*-like taxon	Appendage
KUMIP 204781a/b	5.3, 5.4	Wheeler Formation Cambrian Drumian	*Peytoia nathorsti* *Hurdia*	Conway Morris & Robison, 1988; Daley et al., 2013a	hurdiid	Appendage
KUMIP 312405a/b	3	Spence Shale Cambrian Stage 5	Anomalocarididae gen. et sp. indet.	Briggs et al., 2008	*Hurdia*	Appendage and mouthpart
KUMIP 314039	4.2	Spence Shale Cambrian Stage 5	-	-	*Hurdia victoria*	H-element
KUMIP 314040a/b	2.3, 2.4	Spence Shale Cambrian Stage 5	-	-	*Hurdia*	Appendage
KUMIP 314042	2.5	Spence Shale Cambrian Stage 5	-	-	*Hurdia*	Appendage
KUMIP 314050	4.1, 4.4	Spence Shale Cambrian Stage 5	-	-	*Hurdia victoria*	H-element

KUMIP 314056	4.3, 4.5	Spence Shale Cambrian Stage 5	-	-	*Hurdia victoria*	H-element
KUMIP 314057a/b	4.6, 4.7	Spence Shale Cambrian Stage 5	-	-	*Hurdia*	Flap
KUMIP 314078	5.8, 5.9	Wheeler Formation Cambrian Drumian	Anomalocarididae gen. et sp. indet.	Briggs et al., 2008	*Peytoia nathorsti*	Mouthpart
KUMIP 314086a/b	5.1, 5.2	Wheeler Formation Cambrian Drumian	Anomalocarididae gen. et sp. indet.	Briggs et al., 2008	*Peytoia nathorsti*	Appendage
KUMIP 314095a/b	6.6, 6.7	Marjum Formation Cambrian Drumian	-	-	*Peytoia nathorsti*	Mouthpart
KUMIP 314127	Not figured	Spence Shale Cambrian Stage 5	-	-	hurdiid	Mouthpart
KUMIP 314145a/b	2.1	Spence Shale Cambrian Stage 5	-	-	*Hurdia*	Appendage
KUMIP 314175a/b	2.6	Spence Shale Cambrian Stage 5	-	-	*Hurdia*	Mouthpart
KUMIP 314178	2.2	Spence Shale Cambrian Stage 5	-	-	*Hurdia*	Appendage
KUMIP 314265a/b	2.7	Spence Shale Cambrian Stage 5	-	-	*Hurdia*	Mouthpart
USNM 374593	6, 7	Marjum Formation Cambrian Drumian	*Peytoia nathorsti*	Briggs & Robison, 1984	*Peytoia nathorsti*	Body

Table 2. Locations from which hurdiid specimens are known.

	HCM	Shui.	Balang	Jince	Spence	Tulip	Burg.	Stan.	Wheel.	Marj.	Fez.
***Hurdia* specimens**											
H. victoria H-elements					Y	Y	Y	Y			Y
H. triangulata H-element						Y	Y	Y			
P-element		Y		Y		Y	Y		Y		Y
Appendage					Y	Y	Y	Y			
Oral cones					Y	Y	Y	Y			
App. + Oral cone assem.							Y	Y			
Body (partial/complete)						Y	Y	Y			
Isolated flap					Y						
***Peytoia* specimens**											
Appendage	Y		Y			Y	Y		Y		
Oral cone						Y	Y		Y	Y	
Body (partial/complete)						Y	Y			Y	
Other hurdiid appendages						Y		Y	Y		Y
Publications	1	2	3	4	5,6	7	7	8	5, 6, 9	10	11

Publications: 1=Daley & Legg (2015); 2=Cui and Hou (1990); 3=Lui (2013); 4=Chulpac & Kordule (2002); 5=Conway Morris & Robison (1988); 6=Briggs et al. (2008); 7=Daley & Budd 2010; 8=Caron et al., 2010; 9=Robison & Richards 1981; 10=Briggs & Robison (1984); 11=Van Roy & Briggs (2011).